Dynamic Changes in the Distribution of Minerals in Relation to Phytic Acid Accumulation during Rice Seed Development[1][W]

Toru Iwai, Michiko Takahashi, Koshiro Oda, Yasuko Terada, and Kaoru T. Yoshida*

Graduate School of Agricultural and Life Sciences, The University of Tokyo, Bunkyo-ku, Tokyo 113–8657, Japan (T.I., K.O., K.T.Y.); Faculty of Agriculture, Utsunomiya University, Utsunomiya, Tochigi 321–8505, Japan (M.K.); and Super Photon Ring-8, Japan Synchrotron Radiation Research Institute, Sayo-cho, Sayo-gun, Hyogo 679–5198, Japan (Y.T.)

Phytic acid (inositol hexakisphosphate [$InsP_6$]) is the storage compound of phosphorus in seeds. As phytic acid binds strongly to metallic cations, it also acts as a storage compound of metals. To understand the mechanisms underlying metal accumulation and localization in relation to phytic acid storage, we applied synchrotron-based x-ray microfluorescence imaging analysis to characterize the simultaneous subcellular distribution of some mineral elements (phosphorus, calcium, potassium, iron, zinc, and copper) in immature and mature rice (*Oryza sativa*) seeds. This fine-imaging method can reveal whether these elements colocalize. We also determined their accumulation patterns and the changes in phosphate and $InsP_6$ contents during seed development. While the $InsP_6$ content in the outer parts of seeds rapidly increased during seed development, the phosphate contents of both the outer and inner parts of seeds remained low. Phosphorus, calcium, potassium, and iron were most abundant in the aleurone layer, and they colocalized throughout seed development. Zinc was broadly distributed from the aleurone layer to the inner endosperm. Copper localized outside the aleurone layer and did not colocalize with phosphorus. From these results, we suggest that phosphorus translocated from source organs was immediately converted to $InsP_6$ and accumulated in aleurone layer cells and that calcium, potassium, and iron accumulated as phytic acid salt (phytate) in the aleurone layer, whereas zinc bound loosely to $InsP_6$ and accumulated not only in phytate but also in another storage form. Copper accumulated in the endosperm and may exhibit a storage form other than phytate.

The transport of nutrients into developing seeds has received considerable attention. During the grain-filling stage, plants remobilize and transport nutrients distributed throughout the vegetative source organs into seeds. Plant seeds contain large amounts of phosphorus (P) in organic form, which supports growth during the early stages of seedling development. Most of the P in seeds is stored in the form of phytic acid (inositol hexakisphosphate [$InsP_6$]). Seeds also accumulate mineral nutrients such as potassium (K), magnesium (Mg), calcium (Ca), iron (Fe), zinc (Zn), copper (Cu), and manganese (Mn), which are used in seedling growth. Phytic acid acts as a strong chelator of metal cations and binds them to form phytate, a salt of $InsP_6$ (Lott et al., 2002; Raboy, 2009). During germination, phytate is decationized and hydrolyzed by phytases, and then inorganic phosphates, inositol, and various minerals are released from the phytate (Loewus and Murthy, 2000). Phytate accumulates within protein bodies, generally of vacuolar origin, in seed storage cells and is usually concentrated in spherical inclusions called globoids. Many studies of the elemental composition of phytate in seeds have been published. Energy-dispersive x-ray microanalyses of many plant species have revealed that, other than P, globoids contain mainly K and Mg as well as low levels of Ca, Mn, Fe, and Zn (Lott, 1984; Lott et al., 1995; Wada and Lott, 1997). This indicates that phytate is a mixed salt of these cations.

Whether all storage metal elements can bind equally to $InsP_6$ is not known, although most elements are thought to exist in seeds in the form of phytate (Raboy, 2009). To form phytate, P and the other elements must be present in the same place. Therefore, determination of the precise locations of P and other elements in seed tissues makes it possible to judge whether an element exists in the form of phytate. Differences in metal distribution with P might suggest a storage form other than phytate. For determining distributions, synchrotron-based x-ray microfluorescence (μ-XRF) imaging utilizing an x-ray microbeam is a powerful tool. The microbeam excites the elements, thereby revealing the details of their spatial distribution. The development of focusing optics for high-

[1] This work was supported by Japan Advanced Plant Science Network and the Japan Synchrotron Radiation Research Institute (proposal nos. 2009B1724 and 2010B1695).

* Corresponding author; e-mail ayosida@mail.ecc.u-tokyo.ac.jp.

The author responsible for distribution of materials integral to the findings presented in this article in accordance with the policy described in the Instructions for Authors (www.plantphysiol.org) is: Kaoru T. Yoshida (ayosida@mail.ecc.u-tokyo.ac.jp).

[W] The online version of this article contains Web-only data.
www.plantphysiol.org/cgi/doi/10.1104/pp.112.206573

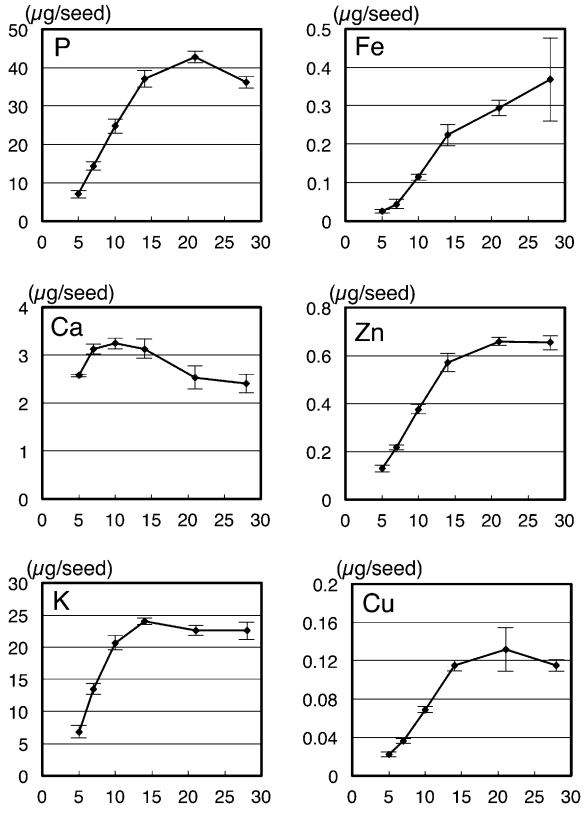

Figure 1. Changes in P, Ca, K, Fe, Zn, and Cu contents during seed development from 5 to 28 DAF. The mineral contents were measured by ICP-OES analysis. Each value represents the mean ± SE of three replicates.

energy x-rays using a Kirkpatrick-Baez mirror raises the imaging resolution of elements in μ-XRF analysis. A focal spot size smaller than 1 μm with x-ray energy as high as 100 keV enables detection of the subcellular distribution of elements in plant tissues (Fukuda et al., 2008; Takahashi et al., 2009).

Whether there is an order in the affinity of elements for phytic acid in plant cells remains unknown. The stability of $InsP_6$-metal complexes has been estimated by in vitro titration (Maddaiah et al., 1964; Vohra et al., 1965; Persson et al., 1998). The binding strength of $InsP_6$ with metal is stronger for Zn and Cu than for Fe, Mn, and Ca. We also do not know if the mineral composition of phytate in seeds is determined by the relative abundance of these elements in the seed or by their biochemical characteristics. As a first step to address these issues, we examined the simultaneous changes in the distribution of P and metal elements during seed development using μ-XRF imaging analysis.

Our objective in this study was to observe the dynamic changes in the distribution of some nutritionally important minerals (P, Ca, K, Fe, Zn, and Cu) in relation to the accumulation of phytic acid during rice (*Oryza sativa*) seed development.

RESULTS

Accumulation of Minerals in Developing Seeds

To determine the accumulation patterns of the minerals during seed development, we performed inductively coupled plasma optical-emission spectrometry (ICP-OES) analysis (Fig. 1). Mineral contents, except Ca, rapidly increased until 14 d after flowering (DAF), as the weight of the seeds increased (Fig. 2). Both the fresh and dry weights of seeds increased from 5 to 21 DAF. Levels of P, Fe, and Zn gradually increased between 14 and 21 DAF. In contrast, the increases in K and Cu contents almost stopped after 14 DAF. The increase in P and Zn halted after 21 DAF, as did the increase in seed weight. The Ca content in developing seeds differed greatly from that of other minerals, being nearly constant from 5 to 28 DAF. The Ca concentration on the basis of seed fresh weight decreased until 21 DAF as the fresh weight of seeds increased (Supplemental Fig. S1).

Phosphate and $InsP_6$ Levels in Developing Seeds

Concentrations of phosphate (Pi) and $InsP_6$ during seed development were determined by ion chromatography (Fig. 3). We separately analyzed the inner starchy endosperm and the outer endosperm containing the aleurone and subaleurone layers. Pi concentration did not change greatly during seed development, being maintained at low levels in both the inner and outer endosperms. In contrast, $InsP_6$ concentration differed greatly between the two parts. The $InsP_6$ level of the inner starchy endosperm remained at low levels (0.3–1.0 mg g^{-1}) from 7 to 30 DAF, whereas that of the outer endosperm increased rapidly from 10 to 25 DAF. No signal peak of inositol phosphates other than $InsP_6$ was detected in these chromatography experiments. These results suggest that Pi is assimilated into $InsP_6$ form immediately following their transfer from vegetative organs to seeds.

After 20 DAF, the levels of Pi decreased slightly in both parts of the endosperm (Fig. 3). By this time, the translocation of P from vegetative organs into seeds had

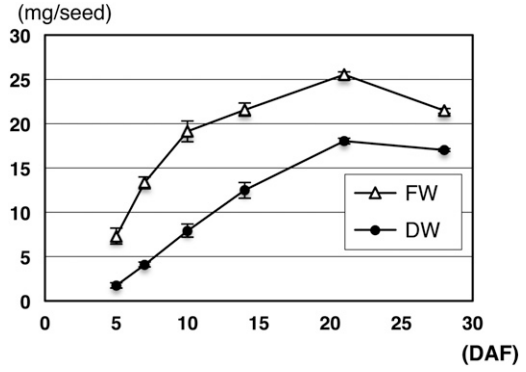

Figure 2. Growth of rice seeds in terms of dry weight (DW; closed circles) and fresh weight (FW; open triangles) from 5 to 28 DAF. Each value represents the mean ± SE ($n > 14$).

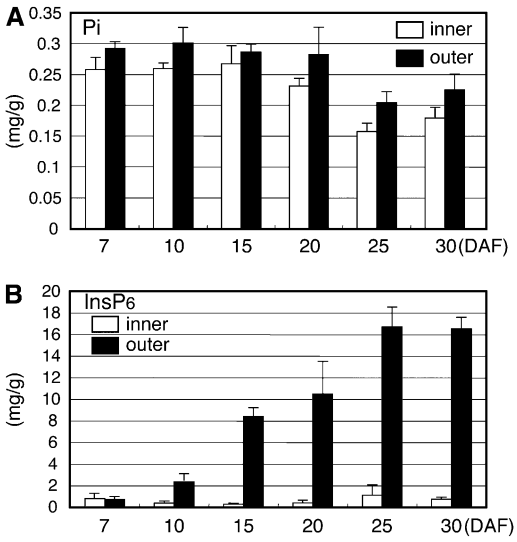

Figure 3. Changes in the Pi (A) and $InsP_6$ (B) contents of inner (white bars) and outer (black bars) endosperms during seed development from 7 to 30 DAF. Pi and $InsP_6$ contents were determined by ion chromatography. Each value represents the mean ± SE of three replicates.

stopped (Fig. 1). Thus, the decrease in Pi contents after 20 DAF might be due to further $InsP_6$ synthesis at this time.

Expression of OsIPK1 in Developing Seeds

The last step in phytic acid synthesis is the phosphorylation of inositol 1,3,4,5,6-pentakisphosphate to $InsP_6$, catalyzed by inositol 1,3,4,5,6-pentakisphosphate 2-kinase (IPK1). Previous studies have revealed that levels of transcripts of the rice *IPK1* homolog gene *OsIPK1* in whole developing seeds increase until 7 DAF and then gradually decrease until 28 DAF (Suzuki et al., 2007). To obtain a general estimation of the localization of phytic acid biosynthesis, we assessed the expression of *OsIPK1* by using reverse transcription (RT)-PCR and immunoblot analyses of immature seeds at 10 and 15 DAF, respectively (Fig. 4). First, we carefully separated the embryo, endosperm, and aleurone layer and then compared the expression levels of OsIPK1 in the three tissues. *OsIPK1* transcripts were detected in the endosperms as well as in the embryos and the aleurone layers (Fig. 4A). OsIPK1 protein was also detected in the endosperms, although protein levels were rather lower in endosperms than in embryos and aleurone layers (Fig. 4B). This suggests that the biosynthesis of $InsP_6$ progresses not only in the aleurone layer and embryo but also in the starchy endosperm. Because chromatography analysis showed $InsP_6$ levels to be consistently low in the inner endosperm during seed development (Fig. 3), $InsP_6$ synthesized in the inner endosperm may immediately transfer to the aleurone layer, or $InsP_6$ synthesis may occur only in the outer endosperm (i.e. in both the aleurone and subaleurone layers) but not in the inner endosperm.

Mineral Distribution Changes during Rice Seed Development

Next, we determined the localization of P, Ca, K, Fe, Zn, and Cu in developing seeds by μ-XRF analysis. Cross sections of the center of freeze-dried immature rice seeds at 10, 15, 20, and 25 DAF were used for x-ray imaging. Figure 5 shows the elemental maps of each element. From 10 to 25 DAF, P accumulated around the aleurone layer and was most abundant on the lateral side of the seed. The localization of Ca, K, and Fe was similar to that of P, as they also accumulated around the aleurone layer during seed development. The differences in Ca, K, and Fe concentrations between the aleurone layer and the inner starchy endosperm were notable. The distribution patterns of the three elements differed somewhat. Ca accumulated uniformly around the aleurone layer, while K, like P, was abundant in the lateral side, and Fe was abundant in the dorsal side, where several vascular bundles, which act as gates for translocation materials, were present.

In contrast, the distribution patterns of Zn and Cu differed from that of P (Fig. 5). Although Zn and Cu were most abundant around the aleurone layer, they were also distributed broadly in the inner endosperm. Cu was abundant on the ventral side near the aleurone layer until 20 DAF. After 20 DAF, Cu spread deeper into the endosperm. Because the translocation of Cu from the vegetative organs was complete before 15 DAF (Fig. 1), this change in localization may depend on the movement of Cu that exists around the aleurone layer. At 25 DAF, Cu was most abundant on the lateral side of the seed. The distribution of Zn changed rapidly during seed development. At 10 DAF, Zn was abundant around the aleurone layer. After 10 DAF, Zn decreased around the aleurone layer and spread into the inner endosperm. Zn exhibited a broader distribution in the endosperm than did Cu and was detected at similar levels in both the central and outer areas of

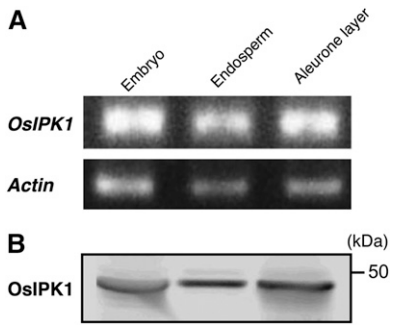

Figure 4. Expression of the *OsIPK1* gene in immature seeds. A, Semiquantitative RT-PCR analysis was performed using total RNAs from the embryo, endosperm, and aleurone layer at 10 DAF. The *Actin* gene was used as an internal control. B, Western-blot analysis was performed using total proteins from the embryo, endosperm, and aleurone layer at 15 DAF.

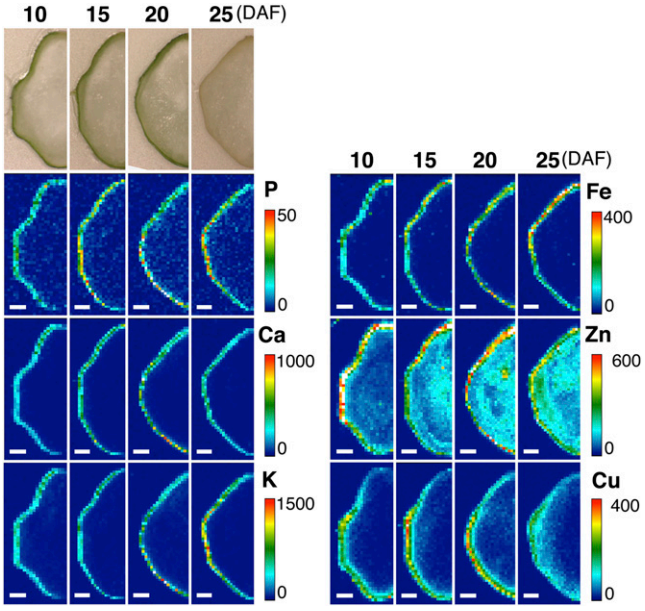

Figure 5. Elemental maps of P, Ca, K, Fe, Zn, and Cu in cross sections of immature seeds at 10, 15, 20, and 25 DAF. Normalized x-ray fluorescence intensities are scaled from red (maximum) to blue (minimum). To generate the maps, a step size of 50 μm was used. Dorsal side is up in all figures. Bars = 300 μm.

the endosperm. Zn was most abundant in the aleurone layer of the dorsal to lateral sides throughout seed development. After 20 DAF, when the translocation of Zn from the vegetative organs had ended (Fig. 1), Zn accumulation around the aleurone layer decreased slightly.

To obtain high-resolution images, we changed the step size of the μ-XRF analysis from 50 μm to 1 μm. At this size, we could compare the exact positions of each element. Figure 6A compares the elemental maps of P, Ca, K, and Fe around the aleurone layer on the lateral side of developing seeds. The distribution areas of Ca, K, and Fe were quite similar to that of P during seed development from 10 to 25 DAF, even though the regions in which each element was most abundant differed slightly. Figure 6B compares the P, Zn, and Cu elemental maps. The distribution of Zn was similar to that of P but was slightly broader, which is apparent in the image at 25 DAF. The Cu accumulation region did not strictly overlap with that of P throughout seed development, and Cu localization changed gradually from 10 to 25 DAF. The area of most abundant Cu moved from the outer to the inner endosperm, and at 25 DAF it was completely different from the site of P localization.

Mineral Localization in Mature Seeds

The distribution patterns of minerals in mature seeds were determined by μ-XRF analysis (Fig. 7). Although the concentrations of each element in the accumulation area increased after 25 DAF (Fig. 5), the localization patterns of these elements did not change markedly (Fig. 7A). P, Ca, K, and Fe accumulated mainly in the aleurone layer. However, Zn and Cu broadly accumulated from the aleurone layer to the inner endosperm. Figure 7B shows the fine elemental maps around the aleurone layer on the ventral side of the seeds as determined by 1-μm step-size analysis. As in the case of developing seeds, the distributions of P, Ca, K, and Fe in the mature seed were similar. The localization sites of these elements were mostly restricted to the aleurone layer. In contrast, Zn and Cu localization differed from that of P, as they were most abundant in the endosperm adjacent to the aleurone layer (i.e. the subaleurone layer).

DISCUSSION

In this study, μ-XRF imaging analysis revealed the dynamic spatial distributions of elements (P, Ca, K, Fe, Zn, and Cu) in developing rice seeds. P accumulated to high levels in the outer cell layers of the endosperm in

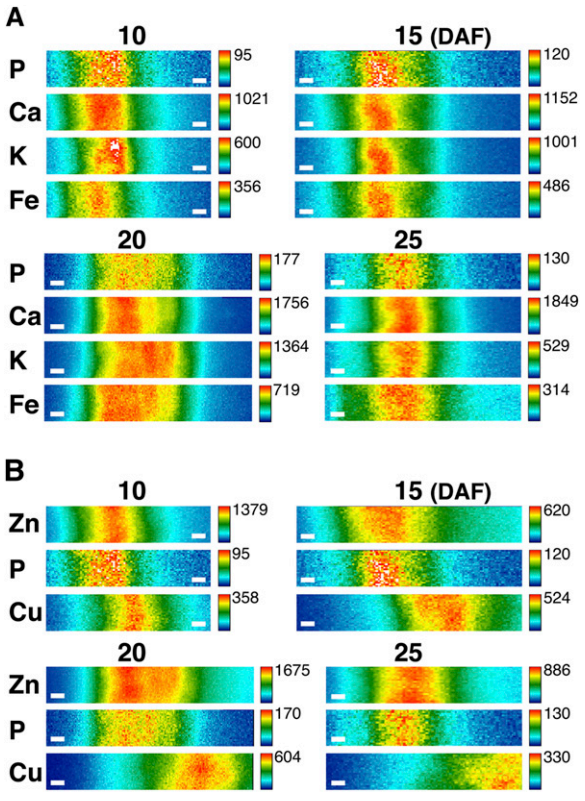

Figure 6. Comparison of elemental maps of Ca, K, Fe, Zn, and Cu with that of P around the aleurone layer on the lateral side of the developing seed from 10 to 25 DAF. A, Comparison of elemental maps of Ca, K, Fe, and P. B, Comparison of elemental maps of Zn, Cu, and P. Normalized x-ray fluorescence intensities are scaled from red (maximum) to blue (minimum). To generate the maps, a step size of 1 μm was used. Dorsal side is up in all images. Bars = 10 μm.

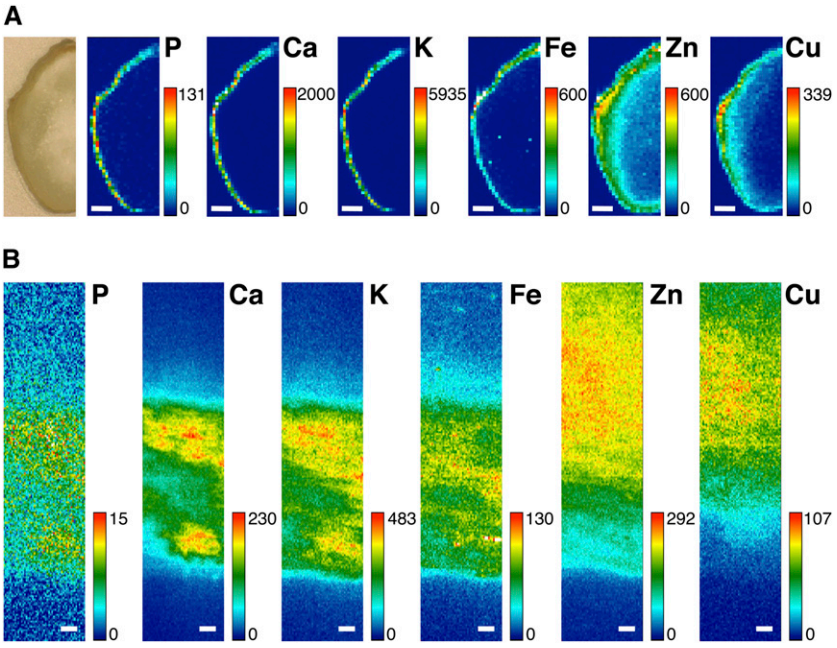

Figure 7. Comparison of P, Ca, K, Fe, Zn, and Cu elemental maps in cross sections of a mature seed. Normalized x-ray fluorescence intensities are scaled from red (maximum) to blue (minimum). A, A cross section of the seed center was used for μ-XRF analysis at 50-μm step size. Bars = 300 μm. B, Elemental maps around the aleurone layer on the ventral side of the seed. To generate the maps, a step size of 1 μm was used. Bars = 10 μm. Dorsal side is up in all figures.

both immature and mature seeds (Figs. 5 and 7). Using ion chromatography, Pi content was determined to be low (0.2–0.3 mg g^{-1}), and inositol phosphates other than $InsP_6$ were not detected in seeds throughout their development. The $InsP_6$ content of the outer endosperm increased rapidly from 10 to 25 DAF (Fig. 3) as P content increased (Fig. 1). Previously, we demonstrated that phytate-containing particles called globoids were present only in the aleurone layer, not in the starchy endosperm, during rice seed development (Yoshida et al., 1999). These results indicate that the majority of P is localized in the aleurone layer as phytic acid throughout seed development. Because translocation of P from vegetative source organs to seeds is active before 21 DAF (Fig. 1), the translocated P is likely converted immediately to $InsP_6$.

OsIPK1 catalyzes the final step of phytic acid biosynthesis from inositol 1,3,4,5,6-pentakisphosphate to $InsP_6$ in rice, and its transcript has been abundant in seeds from 5 to 28 DAF (Suzuki et al., 2007). In this study, *OsIPK1* mRNAs and OsIPK1 proteins were detected not only in the embryos and the aleurone layers, in which the active phytate accumulation was observed, but also in the endosperms. This strongly suggests that phytic acid biosynthesis also occurs in endosperm cells. The concentration of $InsP_6$ in the inner endosperm did not increase, remaining at low levels during seed development from 7 to 30 DAF (Fig. 3). Therefore, $InsP_6$ synthesized in inner endosperm cells may be transported immediately to the aleurone layer, and/or $InsP_6$ synthesis in the endosperm may be restricted to the subaleurone layer.

Using μ-XRF analysis with a 1-μm step size, the subcellular localizations of the elements could be determined. This high-resolution elemental map showed the precise positions of the elements and whether they occupied the same sites. Because the majority of P in the aleurone layer may exist as $InsP_6$, and $InsP_6$ acts as a strong chelator of metal elements, the elements that were detected in the same place as P in the aleurone layer may exist in the form of a phytate salt, making it possible to deduce which elements bind mainly to $InsP_6$. Ca, K, and Fe were restricted mainly to the aleurone layer, and they colocalized with P in both developing and mature seeds. This strongly suggests that Ca, K, and Fe bind to $InsP_6$ in the aleurone layer. In contrast, Zn is more loosely bound to $InsP_6$, because it is localized not only in the aleurone layer but also in the inner endosperm to a considerable extent in immature seeds, and this tendency is stronger in mature seeds. This suggests that Zn binds not only to $InsP_6$ but also to other compounds. Recently, Persson et al. (2009) reported simultaneous detection of Fe, Zn, S, and P in barley (*Hordeum vulgare*) grain using size-exclusion chromatography and ICP-mass spectrometry. Fe and Zn were shown to have a different complex form in barley grain tissues, with Fe associated mainly with P ($InsP_6$) and Zn bound mainly to sulfur (peptides). This conclusion is consistent with our findings. Further research is required to determine the Zn-binding complex during seed development.

Cu localization differed from that of P at almost all seed developmental stages (Figs. 6 and 7), suggesting that Cu binds to a compound other than $InsP_6$. We suggest that translocated Cu passes rapidly through the aleurone layer to the endosperm tissues without being captured by $InsP_6$ in the aleurone layer. The concentration of Cu in seeds is too low to detect using the general method. By means of highly sensitive μ-XRF analysis at Super Photon Ring-8, we can, to our knowledge for the first time, suggest that Cu exists in a storage form other than phytate. In vegetative tissues,

Cu accumulates mainly in chloroplasts and is associated with metalloproteins such as plastocyanin. In spite of the essential role of Cu in plants, Cu ions are highly toxic at elevated concentrations. Therefore, excess cytoplasmic Cu is considered to bind to a detoxification peptide, phytochelatin (Epstein and Bloom, 2004). Further studies are needed to determine whether phytochelatin forms a complex with Cu in seed tissues.

In a study of the solubility and relative stability of various $InsP_6$-metal complexes using potentiometric titration analysis, Vohra et al. (1965) reported that the order of stability was Cu > Zn > nickel > cobalt > Mn > Fe > Ca. Persson et al. (1998) indicated Cu > Zn > cadmium, whereas Maddaiah et al. (1964), using a different titration method, reported the stability order as Zn > Cu > cobalt > Mn > Ca. However, in these studies, Cu and Zn may have had a high affinity for $InsP_6$. In contrast to these in vitro results, in vivo $InsP_6$ is stored mainly with Mg and K in rice and corn (*Zea mays*) seeds (Ogawa et al., 1975; Lin et al., 2005) and with Mg, K, and Ca in wheat (*Triticum aestivum*) seeds (Bohn et al., 2007). In this study, μ-XRF analysis at a 1-μm step size also indicated that Ca, K, and Fe bind strongly to phytic acid, Zn binds loosely, and Cu scarcely binds to phytic acid. The high affinity of Cu and Zn for $InsP_6$ that was found in vitro does not coincide with that observed in the in vivo system.

Nicotianamine (NA) is a chelator of metals and is ubiquitous in higher plants (Curie et al., 2009). The major role proposed for NA is that of a facilitator of long-distance transport of metals in the phloem, and it also has an important role in maintaining metal homeostasis. Fe, Zn, and Cu are likely present as their NA complexes in the phloem (von Wiren et al., 1999). Lee et al. (2009) reported that activation of one of the NA synthase genes, *OsNAS3*, resulted in a significant elevation of Fe, Zn, and Cu contents in rice seeds as well as elevation of NA levels in plants. In contrast, disruption of *OsNAS3* caused the Fe, Zn, and Cu contents of seeds to decrease. These findings suggest that the transport of Fe, Zn, and Cu from source organs into seeds is in the form of NA complexes. After transport into seeds, the elements show the various movements and distributions found in our study. Fe remains primarily in the aleurone layer on the dorsal side. Cu moves immediately into the inner endosperm. Zn stays near the aleurone layer and moves more deeply into the inner endosperm. It has been suggested that Fe and Zn in seeds bind mainly $InsP_6$ and peptides, respectively (Persson et al., 2009). Whether the different movements and distributions of Fe, Zn, and Cu are reflected in differences in the complexes formed by these elements remains to be elucidated.

In this study, Ca content in developing seeds was nearly constant between 5 and 28 DAF (Fig. 1). This is greatly different from the accumulation patterns of the other elements. Ca is considered to move preferentially in xylem and is generally immobile in phloem (Epstein and Bloom, 2004). This is related to the symplastic nature of phloem. The constant Ca contents during seed development suggest that translocation of Ca into a seed via the phloem may be very limited.

Intensive accumulation of seed storage reserves is generally observed during the middle to late stages of seed development (Goldberg et al., 1989). For example, the major storage proteins of rice, glutelins and prolamins, are detected after 10 DAF (Li and Okita, 1993). The onset of phytic acid biosynthesis is unusually early: globoids, phytate-containing particles, have been observed as early as 4 DAF (Yoshida et al., 1999). In this study, we detected active phytic acid accumulation during early seed development, and the concentrations of Pi in seeds were maintained at low levels in both the inner and outer endosperm, which contains the aleurone layer, whereas translocation of P from the vegetative organ into seeds was quite active until 14 DAF (Fig. 1). The accumulation of phytate during the very early stages of seed development must play a role in the developmental process. Plausibly, Pi homeostasis in seed cells is needed throughout seed development, as it is in the vegetative organs. ADP-Glc pyrophosphorylase is a key regulatory enzyme in the biosynthesis of starch (Preiss, 1982). ADP-Glc pyrophosphorylase is allosterically inhibited by Pi in the plant cell (Plaxton and Preiss, 1987). To maintain high starch biosynthesis in endosperm cells throughout seed development, the concentrations of Pi in seed cells must be maintained at low levels. Phytic acid may support active starch synthesis by acting as a reservoir of Pi. Another possible role of phytic acid in early seed development is to protect the seed from oxidative stress. A highly reactive hydroxyl radical is generated from hydrogen peroxide in the presence of Fe by a Fenton or Fenton-like reaction (Prousek, 2007). Reactive species are powerfully toxic oxidants and can damage biomolecules, such as DNA, proteins, and lipids. Phytic acid is one of the natural strong iron chelators and, therefore, may protect seed cells from oxidative stress during seed development. Indeed, Fe was most abundant in the aleurone layer on the dorsal side, which is adjacent to the translocated site (Fig. 5). We suggest that the translocated Fe is immediately captured by phytic acid in the aleurone layer and is prevented from translocating to another location in the seed.

MATERIALS AND METHODS

Plant Materials

Rice (*Oryza sativa* var *japonica*, 'Kitaake' and 'Nipponbare') plants were grown in a greenhouse under natural light in summer. We used only superior caryopses, as growth rates differ between superior and inferior caryopses and seed growth in inferior caryopses is retarded (Kuwano et al., 2009).

ICP-OES Analysis

Immature seeds of Kitaake at 5, 7, 14, 24, and 28 DAF were dehusked and freeze dried. The freeze-dried samples (90–160 mg) were weighed into a glass tube and digested with 500 μL of HNO_3 for 12 h at 80°C on a heat block. Samples were then dissolved with 100 μL of 30% (w/v) hydrogen peroxide and diluted with 0.08 N HNO_3. The concentrations of P, Ca, K, Fe, Zn, and Cu in the acid-digested materials were determined using an ICP-OES apparatus

(model SPS3500; Seiko), according to the manufacturer's instructions. Experiments were repeated three times using three independent seed samples.

Ion Chromatographic Analysis of Pi and $InsP_6$

Immature seeds of cv Nipponbare at 7, 10, 15, 20, 25, and 30 DAF were dehusked, and their embryos were removed. Then, the inner starchy endosperm and the outer endosperm, containing the aleurone and subaleurone layers, were separated using forceps and a razor. The samples were ground with a mortar and pestle after being crushed with Multi-Beads Shocker (Yasui Kikai) and then homogenized in 2.4% HCl. The HCl extracts were subjected to ion chromatography. The details of the extraction and ion chromatography methods have been described previously (Kuwano et al., 2006, 2009). The experiments were repeated three times using three independent seed samples.

RT-PCR Analysis

For RT-PCR analysis, total RNA was prepared from tissues of immature seeds of Nipponbare at 10 DAF. The method of separating the aleurone layer, embryo, and starchy endosperm from seeds at 10 DAF has been described previously (Kuwano et al., 2011). Total RNA was extracted using the RNeasy Plant Mini Kit (Qiagen). Genomic DNA was eliminated by treatment with DNase I, and then the RNA was purified using the RNeasy Micro Kit (Qiagen). RT-PCR amplification was performed using the One-Step RT-PCR Kit (Qiagen). The *Actin* gene was used as the control. The gene-specific primer pairs were 5′-GTGTCTGTTGTATCTTGGTG-3′ and 5′-AAATTCGGCCTACTGCTGAG-3′ for *OsIPK1* and 5′-GAACAACTGGGACGACAT-3′ and 5′-CCTTTGGGTTCA-GAGGAG-3′ for the *Actin* gene.

Immunoblot Analysis

For immunoblot analysis, the separated aleurone layer, embryo, and starchy endosperm from immature seeds of Nipponbare at 15 DAF were used. Samples were crushed with Multi-Beads Shocker, and the powder of samples was defatted with acetone. Then, proteins were extracted from the defatted samples sequentially with solutions A (1 mM EDTA, 1% Triton X-100, 50 mM β-mercaptoethanol, and 10 mM Tris-HCl, pH 7.5) and B (4 M urea, 10% glycerol, 5% β-mercaptoethanol, 2% SDS, and 62.5 mM Tris-HCl, pH 6.5). The extracted proteins were separated by SDS-PAGE and transferred to Immun-Blot polyvinylidene difluoride membranes (Bio-Rad). Each lane contained the proteins extracted from an identical weight of defatted samples. The C-terminal half of the OsIPK1 protein (264 amino acids) produced in *Escherichia coli* was used to raise antibodies in a rabbit. The blotted membranes were incubated with rabbit anti-OsIPK1 antiserum, and the OsIPK1 protein was visualized with goat anti-rabbit IgG alkaline phosphatase conjugate using the ProtoBlot II AP system (Promega) according to the manufacturer's instructions. The experiment was repeated three times using three independent protein samples.

μ-XRF Analysis

cv Kitaake rice seeds were dehusked and freeze dried, cut with a microslicer (Dosaka EM) into 200-μm sections, and subjected to μ-XRF analysis. The μ-XRF imaging analysis was carried out at BL37XU of the Super Photon Ring-8 facility in Hyogo, Japan. Details of the μ-XRF system have been reported by Kamijo et al. (2003) and Hokura et al. (2006). Elemental maps were obtained by scanning the samples with a 10.0-keV monochromatized beam. The monochromatized beam was focused by a Kirkpatrick-Baez mirror system into a 1.0-μm vertical direction $\times$ 1.2-μm horizontal direction microbeam at the sample position. Samples were exposed to the microbeam, and fluorescent x-rays emitted from the samples were detected using a silicon drift solid-state detector. After μ-XRF analysis, we verified the condition of seed samples using an optical microscope and confirmed that there was no obvious microbeam damage to the samples.

To obtain two-dimensional images of P, Ca, K, Fe, Zn, and Cu in the samples, the sample stage was scanned along the *x*-*y* axes during fluorescent x-ray detection. The scanning step size was set to either 50 or 1 μm. X-ray fluorescence intensities were measured for 0.1 s per point. The integrated x-ray fluorescence intensity of each line was calculated from the spectrum and normalized to that of the incident beam, which was measured by an ionization chamber, and then the elemental maps of the measured areas were calculated. X-ray fluorescence intensity in the μ-XRF analysis is directly proportional to the concentration of the element (Terada et al., 2010). The analysis was repeated at least three times using three independent seeds at the same developmental stage.

Sequence data for *OsIPK1* can be found in the Rice Annotation Project Database libraries under accession number Os04g0661200.

Supplemental Data

The following materials are available in the online version of this article.

Supplemental Figure S1. Changes in P, Ca, K, Fe, Zn, and Cu concentrations on the basis of seed fresh weight during seed development from 5 to 28 DAF.

ACKNOWLEDGMENTS

We are grateful to Mr. W. Hosokawa, Mr. G. Kataoka, Mr. H. Kusuda, and Mr. D. Shima for technical assistance with the μ-XRF analysis. We thank the members of Laboratory of Plant Molecular Genetics at the University of Tokyo for comments and participation in discussions.

Received September 4, 2012; accepted October 17, 2012; published October 22, 2012.

LITERATURE CITED

Bohn L, Josefsen L, Meyer AS, Rasmussen SK (2007) Quantitative analysis of phytate globoids isolated from wheat bran and characterization of their sequential dephosphorylation by wheat phytase. J Agric Food Chem **55:** 7547–7552

Curie C, Cassin G, Couch D, Divol F, Higuchi K, Le Jean M, Misson J, Schikora A, Czernic P, Mari S (2009) Metal movement within the plant: contribution of nicotianamine and yellow stripe 1-like transporters. Ann Bot (Lond) **103:** 1–11

Epstein E, Bloom AJ (2004) Mineral Nutrition of Plants: Principles and Perspectives, Ed 2. Sinauer Associates, Sunderland, MA

Fukuda N, Hokura A, Kitajima N, Terada Y, Saito H, Abe T, Nakai I (2008) Micro x-ray fluorescence imaging and micro x-ray absorption spectroscopy of cadmium hyper-accumulating plant, *Arabidopsis halleri* ssp. *gemmifera*, using high-energy synchrotron radiation. J Anal At Spectrom **23:** 1068–1075

Goldberg RB, Barker SJ, Perez-Grau L (1989) Regulation of gene expression during plant embryogenesis. Cell **56:** 149–160

Hokura A, Omuma R, Terada Y, Kitajima N, Abe T, Saito H, Yoshida S, Nakai I (2006) Arsenic distribution and speciation in an arsenic hyperaccumulator fern by x-ray spectrometry utilizing a synchrotron radiation source. J Anal At Spectrom **21:** 321–328

Kamijo N, Suzuki Y, Takano H, Tamura S, Yasumoto M, Takeuchi A, Awaji M (2003) Microbeam of 100 keV x-ray with a sputtered-sliced fresnel zone plate. Rev Sci Instrum **74:** 5101–5104

Kuwano M, Masumura T, Yoshida KT (2011) A novel endosperm transfer cell-containing region-specific gene and its promoter in rice. Plant Mol Biol **76:** 47–56

Kuwano M, Ohyama A, Tanaka Y, Mimura T, Takaiwa F, Yoshida KT (2006) Molecular breeding for transgenic rice with low-phytic-acid phenotype through manipulating *myo*-inositol 3-phosphate synthase gene. Mol Breed **18:** 263–272

Kuwano M, Takaiwa F, Yoshida KT (2009) Differential effects of a transgene to confer low phytic acid in caryopses located at different positions in rice panicles. Plant Cell Physiol **50:** 1387–1392

Lee S, Jeon US, Lee SJ, Kim YK, Persson DP, Husted S, Schjørring JK, Kakei Y, Masuda H, Nishizawa NK, et al (2009) Iron fortification of rice seeds through activation of the nicotianamine synthase gene. Proc Natl Acad Sci USA **106:** 22014–22019

Li X, Okita TW (1993) Accumulation of prolamins and glutelins during rice seed development: a quantitative evaluation. Plant Cell Physiol **34:** 385–390

Lin L, Ockenden I, Lott JNA (2005) The concentrations and distribution of phytic acid-phosphorus and other mineral nutrients in wild-type and *low phytic acid1-1* (*lpa1-1*) corn (*Zea mays* L.) grains and grain parts. Can J Bot **83:** 131–141

Loewus FA, Murthy PPN (2000) *myo*-Inositol metabolism in plants. Plant Sci **150:** 1–19

Lott JNA (1984) Accumulation of seed reserves of phosphorus and other minerals. *In* DR Murray, ed, Seed Physiology, Vol 1, Development. Academic Press, Sydney, pp 139–166

Lott JNA, Greenwood JS, Batten GD (1995) Mechanisms and regulation of mineral nutrient storage during seed development. *In* J Kigel, G Galili, eds, Seed Development and Germination. Marcel Dekker, New York, pp 215–235

Lott JNA, Ockenden I, Raboy V, Batten GD (2002) Phytic acid and phosphorus in crop grains, seeds and fruits. *In* NR Reddy, SK Sathe, eds, Food Phytate. CRC Press, Boca Raton, FL, pp 7–24

Maddaiah VT, Kurnick AA, Reid BL (1964) Phytic acid studies. Proc Soc Exp Biol Med **115:** 391–393

Ogawa M, Tanaka K, Kasai Z (1975) Isolation of high phytin containing particles from rice grains using an aqueous polymer two phase system. Agric Biol Chem **39:** 695–700

Persson DP, Hansen TH, Laursen KH, Schjoerring JK, Husted S (2009) Simultaneous iron, zinc, sulfur and phosphorus speciation analysis of barley grain tissues using SEC-ICP-MS and IP-ICP-MS. Metallomics **1:** 418–426

Persson H, Turk M, Nyman M, Sandberg AS (1998) Binding of Cu^{2+}, Zn^{2+}, and Cd^{2+} to inositol tri-, tetra-, penta-, and hexaphosphates. J Agric Food Chem **46:** 3194–3200

Plaxton WC, Preiss J (1987) Purification and properties of nonproteolytic degraded ADP glucose pyrophosphorylase from maize endosperm. Plant Physiol **83:** 105–112

Preiss J (1982) Regulation of the biosynthesis and degradation of starch. Annu Rev Plant Physiol **33:** 431–454

Prousek J (2007) Fenton chemistry in biology and medicine. Pure Appl Chem **79:** 2325–2338

Raboy V (2009) Approaches and challenges to engineering seed phytate and total phosphorus. Plant Sci **177:** 281–296

Suzuki M, Tanaka K, Kuwano M, Yoshida KT (2007) Expression pattern of inositol phosphate-related enzymes in rice (*Oryza sativa* L.): implications for the phytic acid biosynthetic pathway. Gene **405:** 55–64

Takahashi M, Nozoye T, Kitajima N, Fukuda N, Hokura A, Terada Y, Nakai I, Ishimaru Y, Kobayashi T, Nakainshi H, et al (2009) In vivo analysis of metal distribution and expression of metal transporters in rice seed during germination process by microarray and x-ray fluorescence imaging of Fe, Zn, Mn, and Cu. Plant Soil **325:** 39–51

Terada Y, Homma-Takeda S, Takeuchi A, Suzuki Y (2010) High-energy X-ray microprobe system with submicron resolution for x-ray fluorescence analysis of uranium in biological specimens. X-Ray Opt Instrum **2010:** 317909

Vohra P, Gray GA, Kratzer FH (1965) Phytic acid-metal complexes. Proc Soc Exp Biol Med **120:** 447–449

von Wiren N, Klair S, Bansal S, Briat JF, Khodr H, Shioiri T, Leigh RA, Hider RC (1999) Nicotianamine chelates both FeIII and FeII: implications for metal transport in plants. Plant Physiol **119:** 1107–1114

Wada T, Lott JNA (1997) Light and electron microscopic and energy dispersive x-ray microanalysis studies of globoids in protein bodies of embryo tissues and the aleurone layer of rice (*Oryza sativa* L.) grains. Can J Bot **75:** 1137–1147

Yoshida KT, Wada T, Koyama H, Mizobuchi-Fukuoka R, Naito S (1999) Temporal and spatial patterns of accumulation of the transcript of *myo*-inositol-1-phosphate synthase and phytin-containing particles during seed development in rice. Plant Physiol **119:** 65–72